Energy Conversion and Management: X 13 (2022) 100169

Contents lists available at ScienceDirect

Energy Conversion and Management: X

journal homepage: www.sciencedirect.com/journal/energy-conversion-and-management-x

Energy performance assessment of a novel zeolite-water direct contact adsorptive heat pump for waste heat recovery

Fulvio Buzzi [a], Michelangelo Di Palo [b], Roberto Gabbrielli [a,*]

[a] Dipartimento di Ingegneria Civile e Industriale dell'Università di Pisa, 56126 Pisa, Italy
[b] Glayx Tech Srl, 56025 Pontedera (PI), Italy

ARTICLE INFO

Keywords:
Zeolite
Steam generation
Heat pump
Modelling
Adsorption
Waste heat recovery

ABSTRACT

The adsorption heat pumps are a promising technology suitable for the industrial waste heat recovery. In particular, the direct contact configuration can be used to generate high pressure steam for industrial applications limiting the design complexities. In this paper, a numerical simulation of the adsorption phase of an original configuration of a direct contact water/zeolite heat pump is presented and discussed. Two different models have been developed and compared using experimental data. Different sensitivity analyses were carried out with the aim of understanding the process of steam generation. The mass flow inlet results to be one of the most relevant parameters of the process and, consequently, an innovative process configuration is proposed. A descendent inlet water flow is implemented and compared with the classical ascendent process. The simulations on this configuration demonstrated that it is possible to obtain higher steam production and better process performances doubling the generated steam mass flow.

Introduction

Background

The world primary energy consumption reached 588 GJ in 2018 and more of 80% is due to fossil fuels [1]. The IPCC reports about the necessity to mitigate the climate change highlighting the relevance of the energy efficiency to reduce the fossil fuel consumption [2]. From this point of view, the industrial sector represents a major user of primary energy [3]. The waste heat recovery, together with several strategies (such as: electrification, carbon capture, energy storage, etc.), is an effective tool which can be implemented in order to reduce the industrial greenhouse gas emissions [4].

In the last years, many studies were performed with the aim to investigate different technologies suitable for the industrial waste heat recycle and exploitation. In [5], Ciganda and Cudok presented a now approach to model the absorption heat transformer. The results are validated using a large experimental map obtaining coefficient of performance higher than 0.4 in according with temperature lifts of 55 K. In [6], Cheng et al. investigated the application of several granular materials in the high-temperature waste heat recovery finding various technological issues and research gap. In [7], Simeoni et al. developed a numerical model to simulate the adoption of the waste heat of a steel casting facility for the district heating. They identify a possible win–win solution for both the industry and the citizen. A novel Heat Pipe Thermoelectric Generator (HPTEG) for high temperature waste heat recovery is proposed by Wang et al. in [8]. The pipe performances are investigated for particular conditions obtaining a thermal conductivity 100 times higher than that of copper.

One of the most promising option is to increase the temperature level of the industrial outlet streams using heat pumps in order to recover this large amount of low-enthalpy heat at suitable temperature levels for the industrial applications.

The high-temperature heat pumps are one of the most considered applications in literature for their promising effectiveness for the production of value heat cascades. Mateu-Royo et al. in [9] modelled eight advanced high-temperature heat pump configurations and nine low global warming potential refrigerant fluids to obtain the most optimum solution. In [10], Kosmadakis assessed the waste heat potential in the EU industries underlying the role of the high-temperature industrial heat pumps. Hu et al. in [11] studied an innovative high-efficient industrial waste heat pump capable to reach coefficient of performance close to 5. The heat pumps can be classified into three main groups: vapour compression, absorption and adsorption heat pumps.

The vapour compression is probably the most studied typology of

* Corresponding author.
E-mail address: r.gabbrielli@ing.unipi.it (R. Gabbrielli).

https://doi.org/10.1016/j.ecmx.2021.100169
Received 22 September 2021; Received in revised form 3 December 2021; Accepted 19 December 2021
Available online 23 December 2021

Nomenclature

A	Heat exchange surface, m^2
c	Specific heat, J/kg K
D_{eff}	Effective diffusivity, m^2/s
D	Reactor diameter, m
h	Specific enthalpy, J/kg
$\dot{h}$	Specific enthalpy flow, W/kg
H	Adsorption heat, J/kg
K	Bed permeability, $1/m^2$
K_{LDF}	Mass transfer coefficient, 1/s
L	Reactor height, m
m	Mass, kg
$\dot{m}$	Mass flow, kg/s
p	Pressure, Pa
Q_{out}	External heat exchange, J
R	Specific gas universal constant, Pa•K•m^3/kg
R_p	Zeolite particle radius, m
$\widetilde{R}$	Gas universal constant, J/(mol•K)
s	Reactor thickness, m
S_p	Specific surface area, m^2
t	Time, s
T	Temperature, K
u	Mixture axial velocity, m/s
U	Overall heat exchange coefficient, W/m^2 K
v	Specific Volume, m^3/kg
V	Volume, m^3
x	Uptake, $kg_{water}/kg_{dry\ zeolite}$
x_{eq}	Equilibrium uptake, -
x_{max}	Maximum uptake, -
z	Axial reactor axis, m

Greek symbols

ε	Bed void coefficient, -
ε_p	Zeolite particle void coefficient, -
λ	Latent heat of evaporation, J/kg
μ	Dynamic viscosity, Pa•s
ρ	Density, kg/m^3

Subscripts

case	Reactor structure
evap	Evaporation
i	Generic reactor component
in	Inlet
j	Generic reactor component
liq	Liquid phase
mix	Steam-air mixture
n	Number of reactor components
out	Outlet
p	Constant pressure transformation
steam	Steam phase
sat	Saturation point
sat-liq	Liquid phase saturation point
v	Constant volume transformation
vap	Vapour phase
zeo	Zeolite
zeo,dry	Dry zeolite

heat pump. In [12], Pak and Ri adopted a genetic algorithm to maximize the thermoeconomic effectiveness of steam heat pumps. In [13] Bamigbetan et al. realised a compressive review of the high temperature vapor compression heat pumps. This technology exhibits limits in terms of efficiency and electricity consumption for very high temperature applications [14–15].

The absorption heat pumps reduce the utilisation of electricity, although the low coefficient of performance represents a relevant issue. Moreover, ammonia is usually adopted as working fluid and its toxicity could be important from a safety point of view [16].

The adsorption heat pumps (AHPs) allow to reach high temperature (e.g., 200 °C) using water as working fluid and zeolite as adsorbent bed material [17]. Therefore, the AHPs could be implemented in several industrial processes.

In conclusion, the main advantages and disadvantages of AHPs are summarised below.

Advantages:

- Absence of a compressor.
- Low electricity consumption.
- Adoption of water as working fluid.
- Capability to reach high temperature.

Disadvantages:

- Low overall heat transfer coefficient.
- High heat exchanger complexity.
- Low coefficient of performance.

The AHPs represent a suitable technology for the industrial processes requiring steam water temperature higher than 200 °C, but the research is actually focusing on the low heat exchange performances of these systems.

Literature review

The main challenge about adsorption heat pumps is related to the low heat transfer between the solid adsorbent bed and the working fluid, which has to transfer/collect heat to/from the bed. This is due to the low conductivity of the granular zeolite, which is considered the most suitable material for this kind of application [18]. For this reason, many bed configurations and heat exchanger geometries were proposed and analysed in literature to improve the heat transfer [19–20]. Typically, the solutions are very complex and challenging from the technological point of view.

In order to reduce the project costs and design complexity, in the recent years several experimental and numerical studies were performed considering a direct contact AHP where the adsorbate works also as thermal fluid. In [21], Fukai and Wijayanta evaluated the variation of heat adsorption of the zeolite 13X adsorbent material adopting a cylindrical and spherical shape, while Nakagawa et al. in [22] investigated the combination of a direct contact AHP together with a thermal solar plant at low solar radiation. In [23] and [24], Nakaso et al. analysed in detail the thermodynamic performances of the generation phase from a numerical point of view.

The main difference between an indirect and a direct contact AHP is that the heat exchanger between the solid bed and the working fluid is removed in the direct contact configuration and water (i.e. the industrial thermal cascade) operates at the same time as adsorbate and as thermal fluid to be transformed into steam, which is widely used in industrial process applications as thermal vector. This solution appears quite promising in terms of constructive and operative simplicity and good performances of waste heat exploitation. Up today, the investigation about this novel configuration is quite rare and focused on modelling and testing lab-scale test rig with very small size. In [25], Oktariani et al. demonstrated the feasibility of high-temperature steam production using a direct contact zeolite-water AHP for many experimental conditions. In [26], Xue et al. investigated experimentally the effects of regeneration time on the cyclic steam production. In [27], Xue et al. compared numerical and experimental steam production of the direct contact AHP for different reactor pressures. In [28], Ye et al. examined the benefits of adopting low-enthalpy steam, instead of liquid water, in the first phase of the generation process. Finally, in [29], Xue et al. tested a new composite material as adsorbent bed showing good thermodynamics performances. The numerical analysis of the direct contact AHPs both for generation and regeneration phases were performed by Xue et al. in [30]. A comprehensive explanation of the two-dimensional simulation of the AHP reactors is performed by Oktariani et al. in [31]. The results presented in these works demonstrated the good capability of the AHPs to generate high-temperature steam using simple facilities. The main issue is due to the slow dynamic of generation and regeneration processes.

In the present paper, a numerical analysis of the direct zeolite AHP was carried out with the purpose of examining an innovative configuration of water injection in order to increase the steam production. In particular, according to the work performed by Oktariani et al. in [32], a downdraft water inlet was studied and compared to the updraft configuration.

The innovative feature of this research topic limits the presence of dedicated material in literature. For this reason, the totality of the works performed on this argument are due to a single research group, as can be seen in the references of this article [23–32].

Aims and novel contributions

From the authors' point of view, the advantages due to the adoption of the downdraft configuration were not sufficiently demonstrated and analysed in literature and this paper is focused on this important aspect. Based on authors' knowledge, the Oktariani et al. paper [32] is the only one article published in literature focusing on a direct contact AHP adopting a descendent water inlet flow. The results reported in [32] emphasize the benefits of the adoption of a descent flow reporting an increment of the generated steam of 40% compared to the ascendent flow. Oktariani et al investigated this configuration only from an experimental point of view and not from a numerical one and a limited number of tests are carried out adopting a not uniform radial water injection.

In the present research work, the first numerical analysis on a direct contact AHP with descendent inlet flow is realised, while a uniform radial water injection is implemented investigating the thermodynamic performances. The aim of this article is to fill the literature gap about the descendent inlet flow configuration and to realise a first approach to the numerical simulation of this innovative configuration. In particular, the enhanced heat transfer between the adsorbent bed and the adsorbate is highlighted underlying the consequences in terms of higher steam production and faster generation dynamics when compared with the updraft option. In fact, the descendent flow allows to wet the adsorbent bed more effectively compared to the ascendent configuration requiring a lower amount of feedwater per unit of generated steam. So, considering the large relevance of the application of the zeolite heat pumps for the exploitation of waste heat and direct generation of high value steam for industrial end-users, the aim of this paper is to fill the gap which is present in literature highlighting for the first time the key points and critical aspects of the process thanks a numerical model specifically developed.

The descendent configuration has two main advantages compared to the ascendent one:

1) The overall time of the process is faster thanks to the lower feedwater required.
2) The steam production is higher due to the lower amount of liquid water required for the generation phase. Thus, the medium-temperature liquid water left inside the reactor at the end of the process which contains a large amount of wasted energy is minimized.

From the authors' point of view, the downward flow should be considered as the primary configuration in order to design the direct contact adsorption heat pumps.

The present work is structured in five sections: the second reports a brief description of the process and of the experimental facility presented in [29]. The third explains the numerical models adopted and the assumptions implemented in the simulations. The fourth shows the obtained results while the last chapter reports the conclusions and future remarks.

Description of the direct contact heat pump

The layout of the water/zeolite heat pump for the direct steam generation is reported in Fig. 1. The process is characterised by two phases: steam generation and bed regeneration. In the first one, low temperature water (e.g., 80 °C) is pumped into the reactor from the bottom. The reactor is a stainless-steel cylindrical vessel filled with the adsorbent bed, which is composed by zeolite 13X spherical particles. The contact between the adsorbent bed and the water leads to the occurrence of the adsorption phenomenon. The water adsorption generates the heat of adsorption causing zeolite temperature increase and generation of steam due to the direct contact between the bed and water. Superheated steam exits at the top of the reactor while the zeolite temperature increases due to water adsorption. Finally, the steam mass flow is measured using a flow meter.

In the second phase, hot and dry air is used to regenerate the adsorbent bed. The amount of adsorbed water per unit of mass of dry zeolite is a fundamental parameter of the process defined as water uptake.

The thermodynamic diagram of a typical adsorption cycle is reported in Fig. 2a together with the corresponding simplified reactor scheme (Fig. 2b). The dependence of the adsorbed water per unit of dry zeolite (water uptake) as a function of the zeolite temperature is shown.

A step-by-step description of the cycle process is listed below.

Generation phase:

- Low temperature water (waste heat) enters the reactor (A).
- Water adsorption occurs leading to adsorption heat releases and therefore increasing adsorbent (zeolite 13X) temperature (A-B).
- Water adsorption decreases leading to zeolite temperature reduction (B-C).
- Water uptake reaches the maximum value causing the zeolite temperature decreases (C-D).
- End of the steam generation phase (D).

Regeneration phase:

- Liquid water is drained from the bottom of the reactor (D).
- Ambient pressure hot dry air enters the top of the reactor (D).
- Zeolite adsorbent bed warms up and releases adsorbed water (D-A).
- End of the adsorbent bed regeneration phase (A).

In Fig. 3, the comparison between the simplified scheme of the direct and indirect adsorption heat pump is reported. It can be clearly noted the simpler configuration of the direct design due especially to the absence of the heat exchanger between the operative thermal fluid and the adsorbent bed.

In this work, the experimental results obtained by Xue et al. in [29]

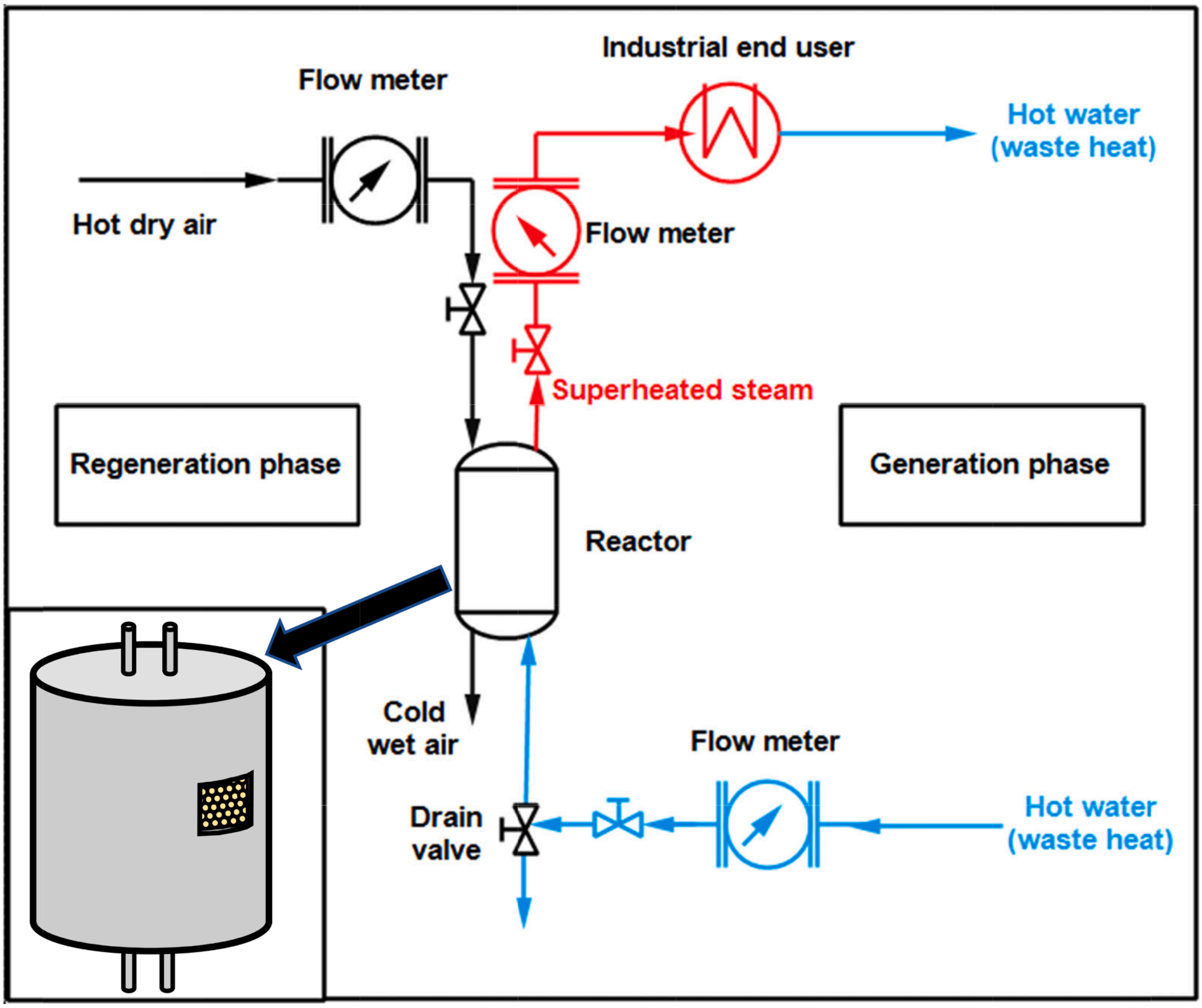

Fig. 1. Simplified scheme of the direct-contact adsorption heat pump and contents/construction of the reactor.

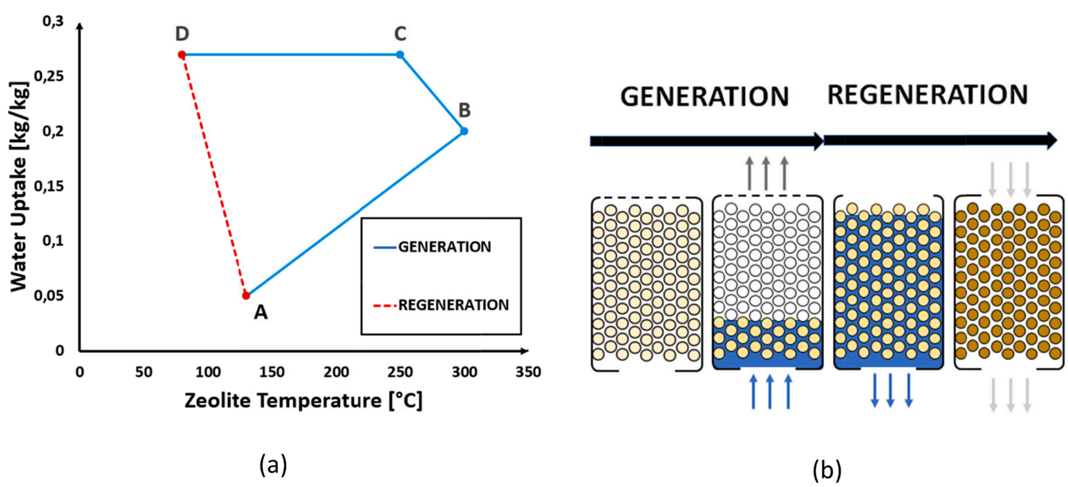

Fig. 2. Thermodynamic diagram of the adsorption cycle (a) and corresponding simplified reactor scheme (b).

were considered to validate the numerical models here developed and to compare experiments and simulations. In particular, a downward water flow inside the reactor was implemented in order to obtain higher steam production compared to the upward flow used in [29]. In fact, the work performed by Oktariani et al. in [32] suggested the possibility to get higher thermodynamic performances adopting a descending flow during the generation phase.

Zeolite is characterised by very low thermal conductivity (e.g., 0.15 W/m K) and for this reason it is suggested to increase the contact surface during the thermal exchange in order to increase the heat transfer. From this point of view, the downward flow allows to achieve a good contact between the adsorbent bed and the adsorbate limiting the effects of low

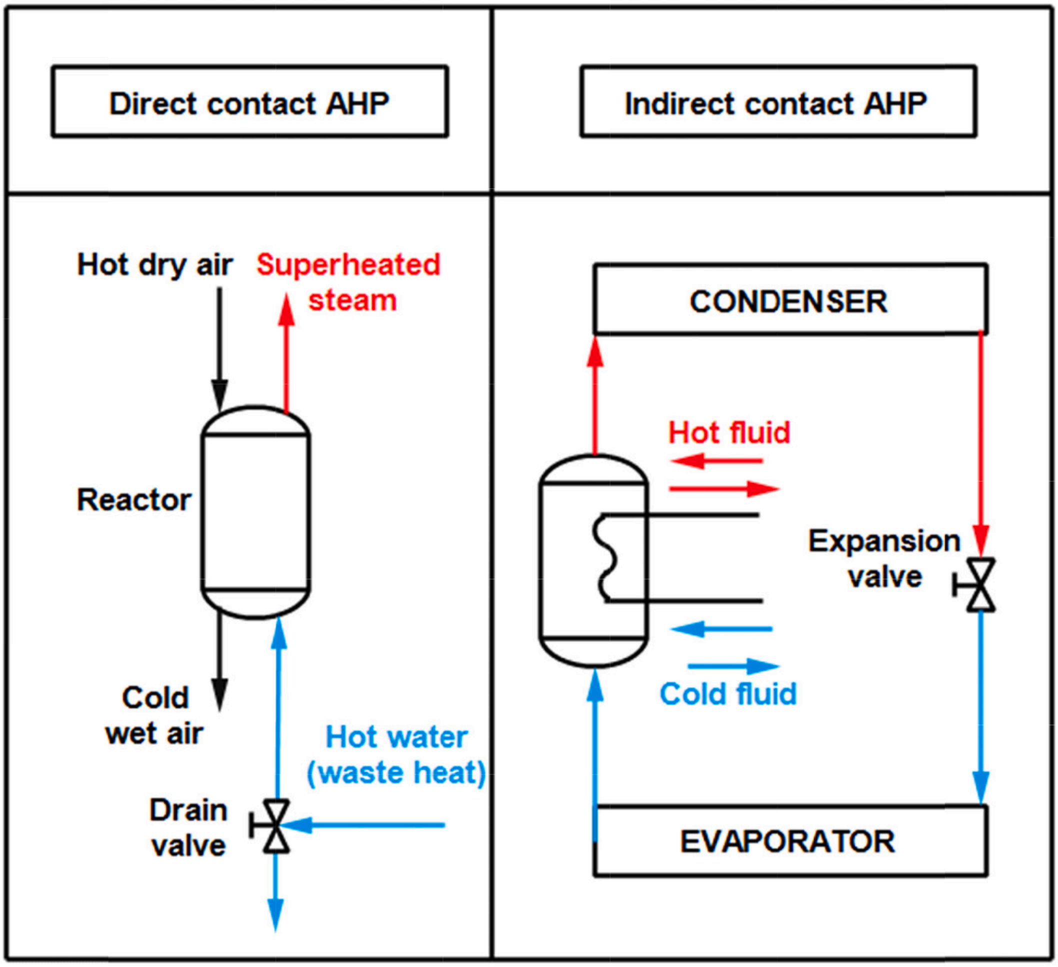

Fig. 3. Comparison between the simplified scheme of the direct and indirect adsorption heat pump.

zeolite thermal conductivity.

Two models of different complexity were implemented in the code in order to analyse the process. The model description is reported in the next section.

Mathematical models of the absorption process

In this paper two different mathematical models of the adsorption process between water and zeolite are presented in the following.

Lumped-parameter model

The lumped model is characterized by parameters that are time-dependent without any spatial dependence. The lumped model is a common and well-known simulation approach usually implemented in literature. Its simplicity and reliability assure high confidence and low computational cost. In particular, this paper adopts the same numerical model presented in the previous work on AHP [20]. The expressions of the time-derivative balance equations are reported below.

Mass balances:

$$\frac{\partial(\rho\bullet V)_{liq}}{\partial t} = \dot{m}_{in} - \dot{m}_{evap} - \left(\frac{\partial x}{\partial t}\right)_{liq} \bullet m_{zeo,dry} \quad \text{(liquid water)} \tag{1}$$

$$\frac{\partial(\rho\bullet V)_{mixture}}{\partial t} = \dot{m}_{evap} - \dot{m}_{out} - \left(\frac{\partial x}{\partial t}\right)_{steam} \bullet m_{zeo,dry} \quad \text{(air-steam mixture)} \tag{2}$$

Energy balances:

$if T_{liq} < T_{sat-liq}$

$$\begin{cases} \dfrac{\partial(\rho\bullet c_v\bullet V\bullet T)_{liq}}{\partial t} = \dot{m}_{in}\bullet h_{in} - \left(\dfrac{\partial x}{\partial t}\right)_{liq}\bullet m_{zeo,dry}\bullet h_{liq} + \sum_i^n U_{i-j}\bullet A_{i-j}\bullet (T_i - T_j) \\ \dot{m}_{evap} = 0 \end{cases} \tag{3}$$

if $T_{liq} = T_{sat-liq}$

$$\begin{cases} \dot{m}_{evap} = \dfrac{\sum_i^n U_{i-j}\bullet A_{i-j}\bullet (T_i - T_j) - \dot{m}_{in}\left(h_{liq} - h_{in}\right)}{\lambda} \\ \dfrac{\partial T_{liq}}{\partial t} = 0 \end{cases} \quad \text{(liquid water)} \tag{4}$$

$$\frac{\partial(\rho\bullet c_v\bullet V\bullet T)_{mix}}{\partial t} = \dot{m}_{evap}\bullet \mathrm{h_{evap}} - \mathrm{\dot{m}_{out}}\bullet \mathrm{h_{out}} - \left(\frac{\partial \mathrm{x}}{\partial \mathrm{t}}\right)_{\mathrm{steam}}\bullet \mathrm{m_{zeo,dry}}\bullet \mathrm{h_{steam}} + \sum_{i}^{n} \mathrm{U_{i-j}}\bullet \mathrm{A_{i-j}}\bullet(\mathrm{T_i}-\mathrm{T_j}) \quad \text{(air-steam mixture) (5)}$$

$$\frac{\partial(\rho\bullet c_v\bullet V\bullet T)_{zeo}}{\partial t} = \left(\frac{\partial \mathrm{x}}{\partial t}\right)_{liq}\bullet \mathrm{m_{zeo,dry}}\bullet \mathrm{H_{liq}} + \left(\frac{\partial \mathrm{x}}{\partial \mathrm{t}}\right)_{\mathrm{steam}}\bullet \mathrm{m_{zeo,dry}}\bullet \mathrm{H_{steam}} + \sum_{i}^{n} \mathrm{U_{i-j}}\bullet \mathrm{A_{i-j}}\bullet(\mathrm{T_i}-\mathrm{T_j}) \quad \text{(zeolite) (6)}$$

$$\frac{\partial(\rho\bullet c_v\bullet V\bullet T)_{case}}{\partial t} = \sum_{i}^{n} U_{i-j}\bullet \mathrm{A_{i-j}}\bullet(\mathrm{T_i}-\mathrm{T_j}) \quad \text{(case) (7)}$$

Ideal gas law:

$$p\bullet \mathrm{v} = \mathrm{R}\bullet \mathrm{T} \quad (8)$$

The heat exchange between the reactor components (i.e., zeolite, liquid water, air–steam mixture and case) is considered adopting an overall heat exchange coefficient $U_{i\text{-}j}$ and the heat exchange contact area $A_{i\text{-}j}$.

Kinetic of adsorption

The zeolite kinetic of both liquid and steam adsorption was analysed in detail in several research articles [33–35]. In fact, the linear driving force (LDF) model was deeply studied and applied in literature thanks to its simplicity and numerical consistence. Results obtained using LDF model were usually in good agreement with experimental ones. The LDF model allows to calculate the uptake time variation as a function of three parameters, as can be seen in the following equation:

$$\frac{\partial x}{\partial t} = K_{LDF}\bullet(\mathrm{x_{eq}} - \mathrm{x}) \quad (11)$$

The mass transfer coefficient K_{LDF} of the model was calculated using the expression in [35] and reported below:

$$K_{LDF} = \frac{15\bullet \varepsilon_p\bullet D_{eff}\bullet p_{vap}}{R_p{}^2\bullet \rho_{zeo}\bullet R\bullet T_{zeo}\bullet x_{eq}} \quad (12)$$

The coefficients of this equation were reported in Table 1 according to [34]. The equilibrium uptake was calculated considering the results presented in [34]. In particular, the Sips model was implemented in the code together with the Aranovich-Donohue correction. The equations of the model are reported below, and the coefficients are presented in Table 1.

Table 1
Simulation parameters implemented in the software for the solving of the kinetic of adsorption.

Parameter	Value	SI unit
ε_p	0.582	–
D_{eff}	$7 \bullet 10^{-7}$	m^2/s
f_0	0.288	–
b_0	$1.353 \bullet 10^{-10}$	kPa^{-1}
R	8.314	J/(mol • K)
E	8150	J/mol
x_{max}	0.29	kg_{water} / $kg_{zeolite}$
d	0.02772	–
H_{liq}	1100	kJ/kg
H_{steam}	3500	kJ/kg

$$x_{eq} = x_{max}\bullet\frac{(\mathrm{b}\bullet \mathrm{p_{vap}})^{\mathrm{f_0}}}{1+(\mathrm{b}\bullet \mathrm{p_{vap}})^{\mathrm{f_0}}}\bullet\frac{1}{\left(1-\frac{\mathrm{p_{vap}}}{\mathrm{p_{sat}}}\right)^{\mathrm{d}}} \quad (13)$$

$$b = b_0\bullet \mathrm{e}^{\left(\frac{\mathrm{E}}{R\bullet \mathrm{T_{zeo}}}\right)} \quad (14)$$

The equilibrium uptake was imposed equal to the maximum uptake for the simulation of the liquid adsorption in according to [27].

Solving procedure of the lumped mathematical model

The software Matlab R2020a was used to simulate the reactor during the generation phase. The balance equations were implemented in the code using a finite difference approach together with the numerical explicit method. This is a system of ordinary derivative equations where temperature and mass values are calculated step by step. The ideal gas equation is used to calculate the reactor pressure while a supplementary derivative equation is required for the kinetic of adsorption.

Some simplified assumptions were applied to this model:

- the heat transfer between the adsorbent bed and the internal walls of the reactor was neglected considering the punctiform contact area due to the supposed ideal spherical geometry of the zeolite particles.
- The air–steam mixture was considered as an ideal gas mixture.
- The heat losses into the external ambient were neglected because the reactor is very well insulated.
- The pressure inside the reactor is uniform and equal to 1 bar at the start of the process. This ambient pressure inside the reactor is obtained imposing an outlet mixture flow calculated applying the ideal gas law to the mixture inside the reactor. In particular, steam generation and temperature increase lead to the increment of the reactor pressure and to generation of the outlet flow. The simulation is characterized by the balance between the internal pressure and the outlet flow: as the pressure rises, the outlet flow increases bringing the pressure back to the ambient value.

The geometry parameters adopted in the simulations are reported in Table 2.

The iterative procedure for the solution of the model can be represented as follows:

Table 2
Geometrical parameters implemented in the simulations.

Parameter	*Value*	*SI unit*
L	0.13	m
D	0.1	m
R_p	0.0011	m
$\rho_{zeo,dry}$	1047	kg/m^3
ε	0.36	–
s	0.002	m

Table 3
Initial and boundary conditions adopted in the simulations.

Parameter	Value	SI unit
$T_{zeo(t=0)}$	130	°C
$T_{mix(t=0)}$	130	°C
$T_{case(t=0)}$	130	°C
$x_{(t=0)}$	0.063	–
p	1	bar
$T_{liq(t=0)}$	80	°C
m_{in}	0.001	kg/s
Q_{out}	0	kJ

1. The initial and boundary conditions are used in the balances to obtain the temperature and mass values at the end of the first iteration.
2. The temperature and mass values are applied to the ideal gas law equation to obtain the new reactor pressure.
3. The difference between the pressures at the time steps 0 and 1 is used to calculate the outlet mixture mass.
4. The outlet flow lowers the reactor pressure to the ambient value.
5. The values at the end of the time step 1 are used to calculate the ones at the time step 2. The iterative procedure is closed.

The initial conditions of the simulation and the boundary conditions are reported in Table 3 according to [29].

Bidimensional model

The bidimensional model can be considered as an evolution of the lumped model. The main advantage is the possibility to calculate the parameters variations as a function of the reactor height (i.e. a spatial coordinate). The axial discretisation was obtained dividing the reactor into several smaller reactors which communicate thanks to the heat and mass transfer. The axial thermal conductivity inside the zeolite was neglected considering the punctiform contact area and the very low zeolite thermal conductivity (i.e., 0.15 W/m K).

The balance equations implemented were in according to the lumped model ones and the main difference is due to the mixture axial flow. The flow axial velocity was calculated in according to the work presented by Oktariani et al. in [26]. In particular, the Darcy equation was applied as reported below.

$$u = -\frac{K}{\mu}\bullet\frac{\partial p}{\partial z} \tag{9}$$

The bed permeability K was obtained using the Kozeny-Carman equation [26].

$$K = \frac{1}{5}\bullet\frac{\varepsilon^3}{(1-\varepsilon)^2}\frac{1}{S_p{}^2} \tag{10}$$

The specific surface area S_p depends on the particle shape and is $3/R_p$

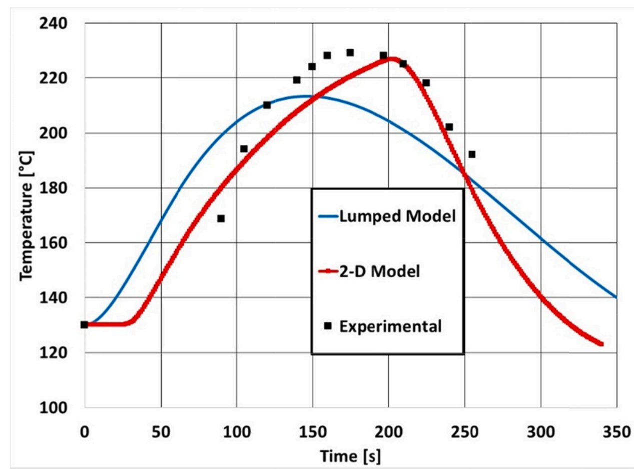

Fig. 5. Temperature trends of the lumped and bidimensional models compared with the experimental measurements.

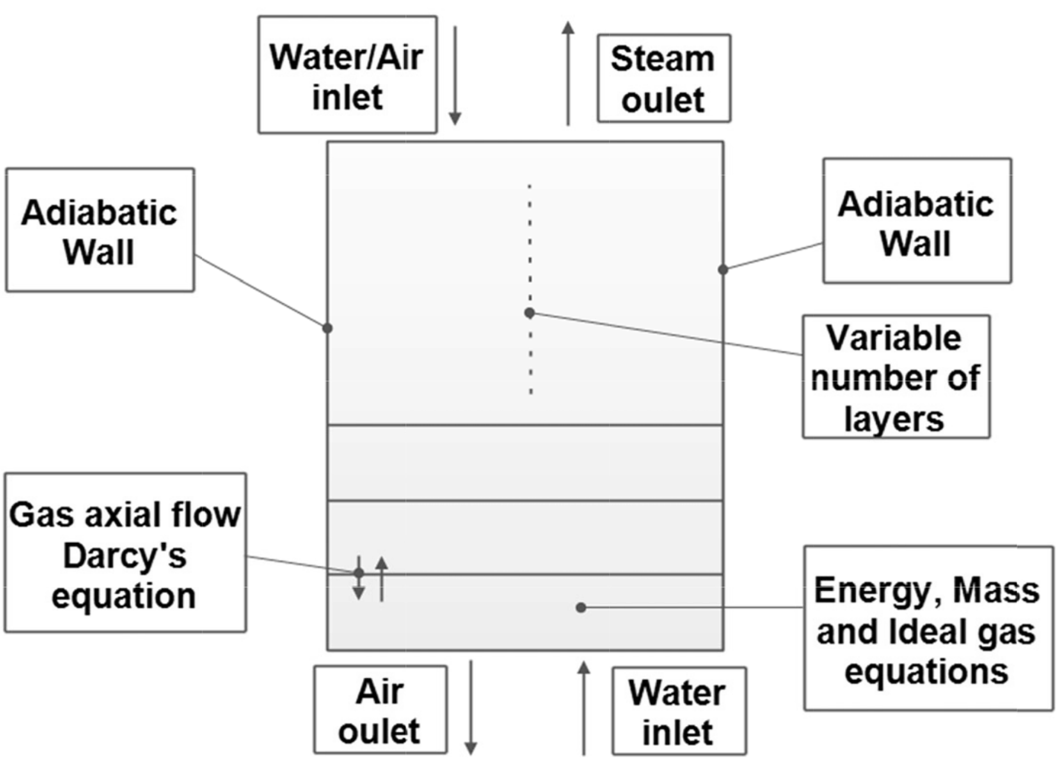

Fig. 4. Computational domain of the two-dimensional model.

for spherical particles, where R_p is the mean radius of the particle. The number of the axial layers can be varied easily in the code, but it is important to adopt a suitable layer thickness. In fact, a low layer height could generate convergence problems and, considering a reactor with an axial size of 0.13 m, a number of layers in the range of 3–7 is suggested.

The iterative procedure is similar to lumped model one, but the outlet mass flow is calculated for the higher layer. The Darcy equation guarantees the axial flow inside the reactor which allows to keep almost constant the pressure inside each layer. The parameters adopted in the bidimensional model equations are reported in Table 3 and the computational domain of the two-dimensional model both for generation and regeneration phase is shown in Fig. 4.

Results

Validation of mathematical models

The experimental results reported in [29] were adopted to validate the present models. The temperature measurements as a function of the time were obtained using a thermocouple placed at one third of the reactor height (accuracy ± 1.5 °C [29]). Fig. 5 shows the comparison between numerical and experimental results

The lumped model exhibits relevant differences compared to the measurements trend. The temperature increase occurs simultaneously to the beginning of the water inlet. This is due to the absence of the axial discretisation; the water adsorption leads to the release of the zeolite adsorption heat and consequently to the uniform bed temperature increment. The temperature peak is achieved before compared to experimental one because the adsorption kinetic is not slowed by the axial distribution. The lumped model is a sort of perfect-contact adsorbent-adsorbate where the adsorption heat is uniformly distributed to the whole zeolite bed which fully participates to the process. In fact, the maximum temperature value is lower compared to experimental one and the general trend is smoother and characterised by slower dynamics.

On the other hand, the bidimensional model shows different results, which are in good agreement with the experimental measurements. In fact, the largest error between numerical and experimental results is in the order of 5%. The initial temperature raise delay is due to the absence of the evaporation in the very first phase of the process. Water enters the reactor at 80 °C and until temperature saturation is not achieved steam generation does not occur. The adsorption heat leads to the increment of the zeolite temperature at the bottom of the reactor, but due to the very low thermal conductivity of zeolite, the temperature in the upper part of the reactor does not increase. As evaporation occurs, the water vapour moves up through the adsorbent bed leading the temperature to sharply raise up. The peak is achieved when the local uptake reaches the maximum value (i.e., wet zeolite). The maximum value is about 230 °C and the total temperature increment during the process is about 100 °C. As the “cold” liquid water arrives in contact with the wet zeolite, the bed temperature dramatically decreases.

It is interesting to note that the temperature of the case changes slightly during the generation process, as can be seen in Fig. 6. This is due to the high steel thermal conductivity and to the absence of contact area with zeolite particles. It can be argued that the structure of the reactor does not contribute to the steam generation.

Sensitivity analyses

The bidimensional model was used to investigate the influence of three parameters on the process performances: inlet water temperature, initial zeolite temperature and water mass flow inlet. These parameters are particularly relevant for the process performances and the assessment of their effects is fundamental for the understanding of the heat pump behaviour.

The lumped model was not considered in these sensitivity analyses due to its low accuracy, according to the results shown in the previous section.

The results obtained were compared with the “standard” test examining the differences in term of steam production. Also the work performed by Xue et al. in [29] is mainly focused on the variation of steam generation for different experimental conditions. Typical heat pump performance indicators, such as the Coefficient Of Performance (COP) or the Gross Temperature Lift (GTL), are not deeply analysed. Considering the novelty of this technology it useful to consider a “concrete” parameter as steam generation in order to optimize the process design.

From the authors’ point of view, it is interesting to realise a comparison between the effect due to zeolite temperature and inlet water temperature in order to estimate which is the most relevant. For this reason, four simulations were performed both increasing and decreasing of 10 °C the initial zeolite temperature and the inlet water temperature, respectively. The steam production for each case is compared with the value of the standard test which is about 0.035 kg [29].

The steam production increments for the different simulations are reported in Fig. 7.

It can be noted that increasing the zeolite and inlet water temperatures obviously lead to a positive increment of the generated steam compared to the standard case. On the opposite, as the temperatures decrease, the steam generation drops. It is important to underline that the influence of the inlet water temperature on the process is higher. The

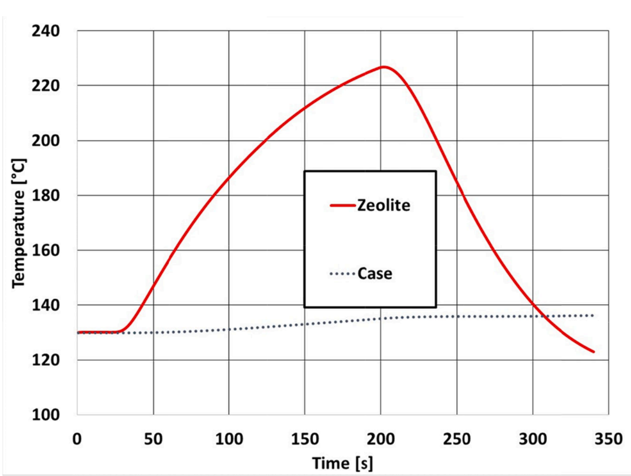

Fig. 6. Zeolite and case temperature trends calculated using the bidimensional model.

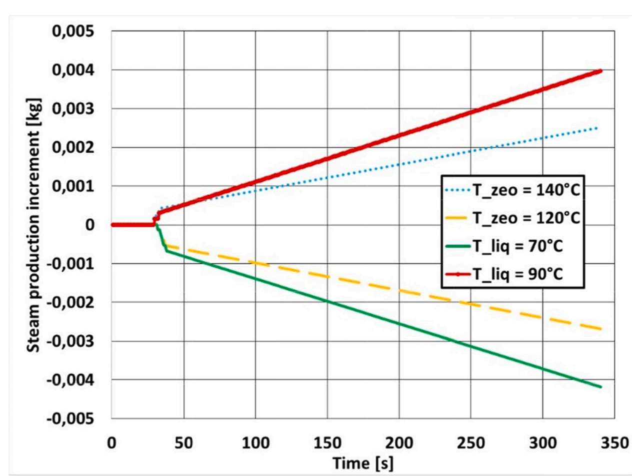

Fig. 7. Steam production increments adopting different zeolite and inlet liquid water temperatures.

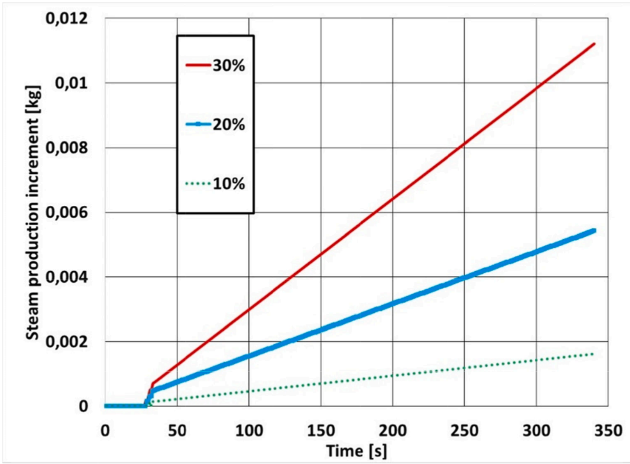

Fig. 8. Steam production increments adopting different inlet mass flow rates.

liquid water specific heat is six time higher than zeolite one and at the end of the generation phase the reactor is full of water. For this reason, increasing the inlet water temperature means higher energy fluxes during the process and consequently larger steam production increments.

It can be argued that the bottom reactor water inlet configuration represents a big issue to deal with. In fact, adopting an ascendent flow requires to fill the reactor of water in order to utilise completely the adsorbent bed. Adopting a higher mass flow inlet can limit this problem increasing the steam production. In Fig. 8, the results of the mass flow inlet sensitivity analysis are reported. The steam production increment compared to the standard case for three different mass flow values is reported. The simulations were realised using a mass flow 10%, 20% and 30% respectively higher than the standard case. It can be noted that this parameter has a huge influence on the process performances underlying the relevance of the inlet flow design.

Downward flow

The main limitation of the adsorption heat pump is due to low thermal heat exchange between the adsorbent bed and the operation fluid. In [19], Pinheiro et al. reported many options useful to increment the heat exchange, such as: complex heat exchangers geometries, different adsorbent-adsorbate pairs, and several bed configurations. The direct contact between zeolite and water allows to reduce the thermal resistances, but the upward flow represents a relevant limitation. The low thermal conductivity and the negligible contact area are the main issues. The spherical geometry of the bed particles is the cause of the pseudo-punctiform contacts between the particles. For this reason, the axial temperature gradient inside the bed adsorbent is very high. In Fig. 9 the temperature trends for the "standard" test for two different axial positions during the generation process are reported.

The lower temperature is calculated at the reactor inlet, while the other one is located two centimetres upper. It can be noted that in the very first phase of the process, the temperature difference is very high and until adsorption occurs at the upper layer, the temperature does not significatively increase. Similar results were found experimentally in many research works, as can be seen in [29]. From this point of view, the axial heat exchange inside the adsorbent bed can be considered negligible. Consequently, it is necessary to fill the reactor with liquid water in order to put in contact the adsorbent with the adsorbate. Steam generation allows to activate the upper part of the reactor, but liquid water must reach the top of the bed in order to exploit the complete adsorption capacity of the adsorbent. In fact, in the experimental applications previous mentioned, the reactor is completely full of liquid water at the end of the generation phase. The experimental facilities presented in literature are characterised by very small reactor, with the total volume of about one litre. In many industrial applications it is necessary to generate high thermal powers and for this reason a larger volume is required. In order to avoid this problem, the work realised by Oktariani et al. in [32] was considered and a downward inlet water flow was tested. The water injection at the top of the reactor allows to easily wet all the adsorbent bed. The experimental test considered is the same reported in the previous paragraph. The initial and boundary conditions were not changed, and the only difference is due to the downward water injection with uniform distribution of water over the transversal section.

In Fig. 10 the temperature trends for the "standard" test for three different reactor positions are reported: bottom, medium and top of the reactor.

It can be noted that there are not sensible differences for the three curves, and this is a relevant issue. The very low reactor height (i.e., 0.13 m) guarantees the immediate drop of the water through the adsorbent bed and consequently the temperature increments occur simultaneously. The reactor peak is lower compared to the upward configuration and this is due to the presence of low temperature liquid water in each layer. On the other side, the steam production is sensible higher compared to upward condition. In Fig. 11, the steam production as a function of time for both upward and downward configuration for the "standard" test and the difference between the two results are reported.

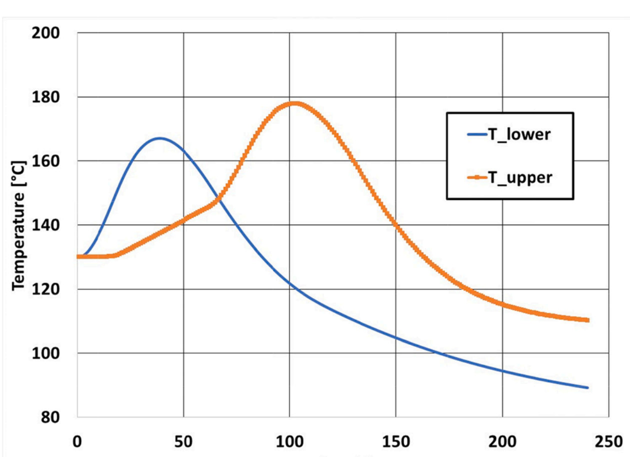

Fig. 9. Temperature trends for two different reactor positions adopting the water inlet upward configuration.

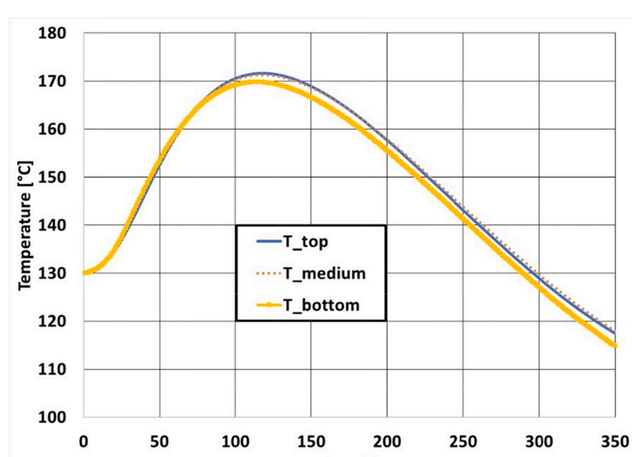

Fig. 10. Temperature trends for three different reactor positions adopting the water inlet downward configuration.

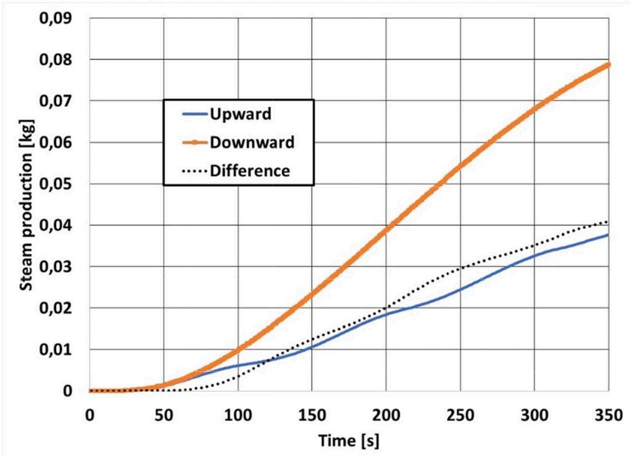

Fig. 11. Steam production and steam production difference of the downward and upward configurations.

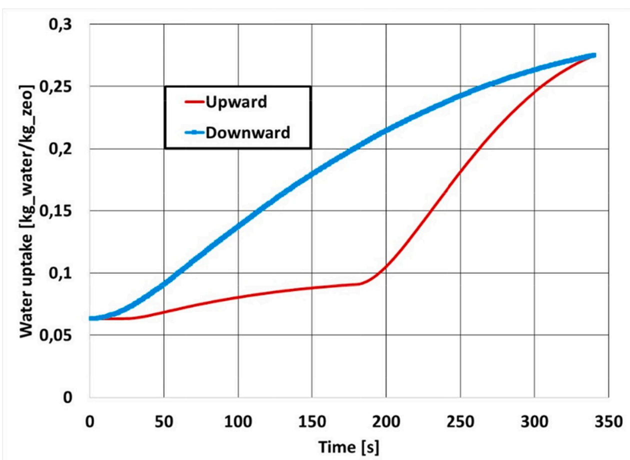

Fig. 12. Water uptake trends adopting the upward and downward configurations.

The steam production increment is higher compared to the steam generated by upward configuration. This means that the steam production is more than double adopting the downward configurations in the first six minutes. After 350 s the steam production tends to zero for the downward configuration, which means that all the adsorption heat is released; this concept is clarified below according to Fig. 12. Otherwise, the upward design is characterised by a longer generation which finishes approximatively after 10 min. This is due to the time required by the water to reach the top of the reactor. According to Fig. 7 and Fig. 8, also for the descendent configuration, similar steam production trends are expected varying inlet water temperature, initial zeolite temperature and inlet water mass flow.

Table 4
Steam production of the downward and upward configurations after 350 s for different boundary conditions.

	Upward	Downward
T_liq = 70 °C	0.034 kg	0.068 kg
T_liq = 90 °C	0.042 kg	0.085 kg
T_zeo = 120 °C	0.035 kg	0.071 kg
T_zeo = 140 °C	0.041 kg	0.081 kg
Inlet mass flow rate 10% higher than standard case	0.040 kg	0.080 kg
Inlet mass flow rate 20% higher than standard case	0.044 kg	0.089 kg
Inlet mass flow rate 30% higher than standard case	0.050 kg	0.101 kg

In Fig. 12, the trends of the water uptake for the two analysed configurations for the “standard” test are reported.

The curves are obtained for a layer placed at one third of the reactor height. It can be noted that the water adsorption occurs immediately for the downward configuration, while the upward one shows two different regions. In the first one the adsorption is due to the steam generation from the lower layers. The amount of generated vapour is low and consequently the uptake increase is limited. During this phase, the temperature of the layer increases sharply because the absence of cold liquid water. The second region is characterised by the contact between the liquid and the zeolite: the slope of the water curve is higher and consequently also the heat of adsorption and the steam generation. On the opposite, the zeolite temperature is characterised by a rapid drop as reported in Fig. 5. At the end of the generation phase, the total amount of steam generated is 80% higher for the downward configuration and the generation time is about 40% lower. The time reduction is due to the immediate contact between zeolite and water guaranteed by the downward flow. The steam increment is mainly caused by the reduction of the total amount of liquid water fed into the reactor during the generation process. In fact, reducing the generation time allows to proportionally reduce the inlet water resulting in a lower quantitative of liquid at the end of the process. The purpose of this heat pump is to generate steam and from this point of view, the liquid water represents a sort of parasite effect. The overall heat of adsorption which is available from the zeolite is a finite quantitative and the hot water inside the reactor represents a loss from the thermodynamic point of view. Therefore, the top water injection assures simultaneously two benefits: time generation reduction and higher steam generation.

In Table 4 the comparison between upward and downward steam production for several cases are reported. The boundary conditions adopted are the same of the previous paragraph and the results agree with the ones shown in Fig. 11: the downward configuration exhibits double steam production.

Industrial application

The direct contact adsorption heat pump can be considered as a prototype technology. As a consequence, the AHPs presented in literature are characterised by very small dimension in terms of volume and thermal power. The typical size of the reactor is about one litre and the generated steam mass flow rate is in the order of magnitude of few tens of grams per hour. The industrial applications require steam mass flow hundreds or thousands time higher and consequently larger reactor size [19]. As a drawback, the more the volume increases, the more the water distribution inside the reactor in not uniform. In fact, considering a 100 L cylindrical reactor with a height of 0.8 m, the diameter should be at less 0.4 m, which is four time higher compared to the geometry considered in this paper. The adoption of many reactors working in parallel could reduce this problem also limiting the steam generation intermittence due to the presence of the regeneration phase. Nevertheless, some industrial applications, which involve very high thermal power, need relevant AHPs volumes. For this reason, it is necessary to investigate the thermodynamics behaviour of large reactor, but the absence of experimental data represents a big issue to deal with. The purpose of the authors is to devote the future works related to this technology to the experimental and numerical analyses of industrial applications. On the other hand, this technology could be associated to many industrial sectors such as: paper production, agri-food, chemical, heating, etc. In general, all the processes accountable of low-temperature waste heat generation and steam production could be a potential application for this AHP. From this point of view, the size of the AHP is not a relevant issue adopting an integrated operation with a conventional boiler. The main purpose is to reduce the utilisation of fossil fuel assuring an economical benefit compared to conventional technologies such as heat exchangers and other typologies of heat pumps. Further analyses and several studies are required in the future in order to investigate the potential of this AHP.

Conclusions

This paper presents a deep investigation about a novel direct contact adsorption heat pump using lumped and bidimensional models.

The comparison between numerical and experimental results shows good agreement for the bidimensional model. On the other hand, the lumped model tends to estimate lower temperature peaks and slower temperature increases. For this reason, the lumped model was not used to perform the other simulations.

A sensitivity analyses was realised in order to investigate the influence of three relevant parameters on the process performances. The obtained results show that the influence of the inlet water temperature on the steam production is higher compared to the initial zeolite temperature one. Otherwise, the mass flow inlet is the most relevant parameter suggesting the importance of the water inlet design. For this reason, a different inlet water flow configuration was tested.

A descendent water flow was simulated and compared to the ascendent one. The downward flow facilitates the contact between the adsorbent and the adsorbate realising a faster generation process. The obtained results clearly demonstrated that the downdraft flow of water is the most effective way to obtain a relevant increase of steam production making the direct water/zeolite heat pump very interesting for the industrial applications.

The present article represents the first study focusing on the numerical simulation of a direct contact AHP with an inlet flow descent configuration. An experimental work realised by Oktariani et al. in [32] demonstrated the potential of this design compared do the ascendent flow. The results reported in this paper confirm this trend showing up to a double steam production. It is authors' opinion that the descent flow should be considered as the preferable configuration in the design of direct-contact adsorption heat pumps, which are characterized by promising performances..

The main limitation of the present model is the absence of the radial and circumferential parameter dependences. Indeed, the water/steam velocity could have a radial component in correspondence of the inlet and outlet. In order to investigate in detail the actual distribution of the working fluid within the zeolite bed and the thermo-fluid-dynamics behaviours of the analysed process, it is necessary to develop further works using a three-dimensional time-dependent simulation approach.

CRediT authorship contribution statement

Fulvio Buzzi: Conceptualization, Methodology, Investigation, Software, Validation, Visualization, Writing – original draft, Writing – review & editing. **Michelangelo Di Palo:** Conceptualization, Resources, Writing – review & editing. **Roberto Gabbrielli:** Conceptualization, Methodology, Investigation, Visualization, Writing – original draft, Writing – review & editing, Funding acquisition.

Declaration of Competing Interest

The authors declare that they have no known competing financial interests or personal relationships that could have appeared to influence the work reported in this paper.

References

[1] https://www.iea.org/world (visited in April 2021). International Energy Agency website.
[2] https://www.ipcc.ch/site/assets/uploads/sites/2/2019/02/SR15_Chapter2_Low_Res.pdf (visited in April 2021). Intergovernmental Panel on Climate Change website.
[3] Urban KL, Scheller F, Bruckner T. Suitability assessment of models in the industrial energy system design. Renew Sustain Energy Rev 2021;137:110400. https://doi.org/10.1016/j.rser.2020.110400.
[4] Jouhara H, Khordehgah N, Almahmoud S, Delpech B, Chauhan A, Tassou SA. Waste heat recovery technologies and applications. Therm Sci Eng Prog 2018;6:268–89.
[5] Corrales Ciganda JL, Cudok F. Performance evaluation of an absorption heat transformer for industrial heat waste recovery using the characteristic equation. Appl Therm Eng 2021;193:116986. https://doi.org/10.1016/j.applthermaleng.2021.116986.
[6] Cheng Z, Tan Z, Guo Z, Yang J, Wang Q. Technologies and fundamentals of waste heat recovery from high-temperature solid granular material. Appl Therm Eng 2020;179:115703.
[7] Simeoni P, Ciotti G, Cottes M, Meneghetti A. Integrating industrial waste heat recovery into sustainable smart energy systems. Energy May 2019;175(15):941–51.
[8] Wang C, Tang S, Liu X, Su GH, Tian W, Qiu S. Experimental study on heat pipe thermoelectric generator for industrial high temperature waste heat recovery. Appl Therm Eng 2020;175:115299. https://doi.org/10.1016/j.applthermaleng.2020.115299.
[9] Mateu-Royo C, Arpagaus C, Mota-Babiloni A, Navarro-Esbrí J, Bertsch SS. Advanced high temperature heat pump configurations using low GWP refrigerants for industrial waste heat recovery: A comprehensive study. Energy Convers Manage 2021;229:113752. https://doi.org/10.1016/j.enconman.2020.113752.
[10] Kosmadakis G. Estimating the potential of industrial (high-temperature) heat pumps for exploiting waste heat in EU industries. Appl Therm Eng 2019;156(25):287–98.
[11] Hu B, Liu H, Wang RZ, Li H, Zhang Z, Wang S. A high-efficient centrifugal heat pump with industrial waste heat recovery for district heating. Appl Therm Eng 2017;125:359–65.
[12] Pak TC, Ri YC. Optimum designing of the vapor compression heat pump using system using genetic algorithm. Appl Therm Eng 2019;147(25):492–500.
[13] Bamigbetan O, Eikevik TM, Nekså P, Bantle M. Review of vapour compression heat pumps for high temperature heating using natural working fluids. Int J Refrig 2017;80:197–211.
[14] Bergamini R, Jensen JK, Elmegaard B. Thermodynamic competitiveness of high temperature vapor compression heat pumps for boiler substitution. Energy 2019;182:110–21.
[15] Luo B, Zou P. Performance analysis of different single stage advanced vapor compression cycles and refrigerants for high temperature heat pumps. Int J Refrig 2019;104:246–58.
[16] Wu W, Wang B, Shi W, Li X. An overview of ammonia-based absorption chillers and heat pumps. Renew Sustain Energy Rev 2014;31:681–707.
[17] Dias JMS, Costa VAF. Adsorption heat pumps for heating applications: A review of current state, literature gaps and development challenges. Renew Sustain Energy Rev 2018;98:317–27.
[18] Demir H, Mobedi M, Ülkü S. A review on adsorption heat pump: Problems and solutions. Renew Sustain Energy Rev 2008;12(9):2381–403.
[19] Pinheiro JM, Salústio S, Rocha J, Valente AA, Silva CM. Adsorption heat pumps for heating applications. Renew Sustain Energy Rev 2020;119:109528. https://doi.org/10.1016/j.rser.2019.109528.
[20] Di Palo M, Sabatelli V, Buzzi F, Gabbrielli R. Experimental and numerical assessment of a novel all-in-one adsorption thermal storage with zeolite for thermal solar applications. Appl Sci 2020;10(23):8517. https://doi.org/10.3390/app10238517.
[21] Fukai J, Wijayanta AT. Potential ability of zeolite to generate high-temperature vapor using waste heat. AIP Conf Proc 2018;1931:020001.
[22] Nakagawa T, Nishi T, Notoji Yu. Development of adsorption steam generator from warm water. J Green Eng 2014;4(2):135–48.
[23] Nakaso K, Tanaka Y, Eshima S, Kobayashi S, Fukai J. Performance of a novel steam generation system using a waterzeolite pair for effective use of waste heat from the iron and steel making process. ISIJ Int 2015;55(2):448–56.
[24] Nakaso K, Eshima S, Fukai J. Generation of high-temperature steam from unused thermal energy by a novel adsorption heat pump. AIP Conf Proc 2017;1788:020004.
[25] Oktariani E, Noda A, Nakashima K, Tahara K, Xue B, Nakaso K, et al. Potential of a direct contact adsorption heat pump system for generating steam from waste water. Int J Energy Res 2012;36(11):1077–87.
[26] Xue B, Iwama Y, Tanaka Y, Nakashima K, Wijayanta AT, Nakaso K, et al. Cyclic steam generation from a novel zeolite–water adsorption heat pump using low-grade waste heat. Exp Therm Fluid Sci 2013;46:54–63.
[27] Xue B, Meng X, Wei X, Nakaso K, Fukai J. Dynamic *study of steam generation from low-grade waste heat in a zeoliteewater adsorption heat pump*. Appl Therm Eng 2015;88:451–8.
[28] Ye S, Xue B, Meng X, Wei X, Nakaso K, Fukai J. Experimental study of heat and mass recovery on steam generation in an adsorption heat pump with composite zeolite-$CaCl_2$. Sustainable Cities and Society 2020;52:101808. https://doi.org/10.1016/j.scs.2019.101808.
[29] Xue B, Ye S, Zhang L, Wei X, Nakaso K, Fukai J. High-temperature steam generation from low-grade waste heat from an adsorptive heat transformer with composite zeolite-13X/$CaCl_2$. Energy Convers Manage 2019;186:93–102.
[30] Xue B, Tahara K, Nakashima K, Noda A, Oktariani E, Wijayanta AT, et al. Numerical Simulation for Steam Generation Process in a Novel Zeolite-Water Adsorption Heat Pump. J Chem Eng Jpn 2012;45(6):408–16.
[31] Oktariani E, Nakashima K, Noda A, Xue B, Tahara K, Nakaso K, et al. T*he feasibility of desorption on Zeolite-water pair using dry gas*. IOP Conference Series: Materials Science and Engineering 2018;344:012002.

[32] Oktariani E, Tahara K, Nakashima K, Noda A, Xue K, Wijayanta ATB, et al. Experimental investigation on the adsorption process for steam generation using a zeolite-water system. J Chem Eng Jpn 2012;20.

[33] Gaeini M, Zondag HA, Rindt CCM. Effect of kinetics on the thermal performance of a sorption heat storage reactor. Appl Therm Eng 2016;102:520–31.

[34] Son KN, Richardson TMJ, Cmarik GE. Equilibrium Adsorption Isotherms for H_2O on Zeolite 13X. Journal of Chemical Engineering Data 2019;64:1063–71.

[35] Gorbach A, Stegmaier M, Eigenberger G. *Measurement and Modeling of Water Vapor Adsorption on Zeolite 4A—Equilibria and Kinetics.* Institut fur Chemische Verfahrenstechnik, Boblinger Straße 72, 70199 Stuttgart, Germany.